Human Molecular Genetics, 2019, Vol. 28, No. 18 3137–3147

doi: 10.1093/hmg/ddz149
Advance Access Publication Date: 17 July 2019
General Article

GENERAL ARTICLE

A gene regulatory network explains *RET–EDNRB* epistasis in Hirschsprung disease

Sumantra Chatterjee† and Aravinda Chakravarti*

Center for Human Genetics and Genomics, New York University School of Medicine, New York, NY 10016, USA.

*To whom correspondence should be addressed at: Center for Human Genetics and Genomics, New York University School of Medicine, 435 East 30th Street, Room 802/3, New York, NY 10016, USA. Tel: +1 212 263 8023; Email: aravinda.chakravarti@nyulangone.org

Abstract

Disruptions in gene regulatory networks (GRNs), driven by multiple deleterious variants, potentially underlie complex traits and diseases. Hirschsprung disease (HSCR), a multifactorial disorder of enteric nervous system (ENS) development, is associated with at least 24 genes and seven chromosomal loci, with *RET* and *EDNRB* as its major genes. We previously demonstrated that *RET* transcription in the ENS is controlled by an extensive GRN involving the transcription factors (TFs) RARB, GATA2 and SOX10 and other HSCR genes. We now demonstrate, using human and mouse cellular and animal models, that *EDNRB* is transcriptionally regulated in the ENS by GATA2, SOX10 and NKX2.5 TFs. Significantly, *RET* and *EDNRB* expression is regulated by their shared use of GATA2 and SOX10, and in turn, these TFs are controlled by *EDNRB* and *RET* in a dose-dependent manner. This study expands the ENS development GRN to include both *RET* and *EDNRB*, uncovers the mechanistic basis for *RET–EDNRB* epistasis and emphasizes how functionally different genes associated with a complex disorder can be united through a common GRN.

Introduction

Although complex traits and disorders have now been shown to comprise small genetic effects at many loci, by genome-wide association (GWAS) and sequencing studies, there is no unifying hypothesis explaining why a particular constellation of genes affects a specific trait (1,2). Some studies attempt to search for enrichment of different functions or pathways among the candidate genes at GWAS loci, but these analyses explain only a minority of the genes or show enrichment for very general protein functions (3,4). Boyle and colleagues have suggested instead that functional networks are shallow, each gene being transcriptionally connected to many genes and being broadly expressed across many cell types (4). Thus, GWAS can fail to distinguish between "core" genes affecting the biology of a trait and "peripheral" genes whose activity are altered as a collateral consequence. A significant task is, therefore, to uncover the core gene regulatory network (GRN) underlying a trait or disease (2). GRNs are modular, comprised of a small number of subcircuit classes and are conserved (5,6), and as we have previously demonstrated, the majority of the genes in core GRNs can be enriched in human disease (7).

In a recent study (7), we deciphered the core enteric GRN underlying Hirschsprung disease (HSCR; congenital intestinal aganglionosis), which is a severe, common (~15/100 000 live births) developmental disorder of the enteric nervous system (ENS) in which the gut fails to be innervated. Genetic studies have identified rare coding variants in 24 genes along with common enhancer variation in two genes and large copy number changes at seven loci to explain the genetic basis of 72% of HSCR cases (8). The features common to these HSCR genes are that they are expressed in the ENS and appear to regulate early differentiation of enteric neural crest cells (ENCCs) into enteric neurons and their subsequent proliferation and migration along

†Sumantra Chatterjee, http://orcid.org/0000-0002-5076-1698
Received: December 31, 2018. **Revised:** May 22, 2019. **Accepted:** June 21, 2019

the gut. Among these, the two most HSCR genes contributing to the greatest susceptibility encode *RET*, a receptor tyrosine kinase, and *EDNRB*, a G protein coupled receptor (9). These two genes are epistatic, in human patients as well as in mouse models of aganglionosis (10–12). The molecular mechanism of this interaction is unknown but important to decipher for understanding the role of early ENS development in HSCR and how *EDNRB* is related to the *RET* GRN.

Genetic control of gene expression is mediated through multiple *cis*-regulatory elements (CREs) and enhancers, which bind specific transcription factors (TFs) organized within a topologically associating domain (TAD) (13,14). Starting with a core TAD and gut-specific epigenomic marks, we have previously deciphered the *RET* GRN and demonstrated that disruption of *RET* enhancer function leads to variable loss of *RET* function and disruption of its enteric GRN (7). Given the strong epistasis between *RET* and *EDNRB*, we, therefore, asked whether genetic control of *EDNRB* shared components with the *RET* GRN. Here, we first identify five enhancers for enteric *EDNRB* gene expression and show that two of these bind GATA2 and NKX2.5; further, the *EDNRB* promoter binds SOX10. Second, by using cellular and animal models, we demonstrate that *GATA2* and *SOX10* are subject to transcriptional feedback by *EDNRB* in a dosage-sensitive manner. Thus, common transcriptional control of *RET* and *EDNRB* by GATA2 and SOX10 and common feedback on these two TFs is the most parsimonious explanation of *RET*–*EDNRB* epistasis. Shared genetic control is, however, insufficient for *RET* and *EDNRB* gene expression because these genes are uniquely controlled by RARB and NKX2.5, respectively (7). This study demonstrates how two major genes in ENS development are functionally regulated via a single GRN and how dose-dependent interactions within this GRN are fundamental to HSCR susceptibility.

Results

EDNRB gut enhancers

To identify *cis*-regulatory elements, we searched for DNase I hypersensitive (DHS), H3K4me1 and H3K27ac sites within a 341 kb (Chr13:78359528-78 701 413) TAD containing *EDNRB* and common to seven human cell lines (GM12878, HMEC, HUVEC, IMR90, K562, KBM7 and NHEK) (14). Candidate *EDNRB* human fetal gut enhancers were identified at 11 regions using NIH Epigenomics Roadmap Consortium data from a 108-day-old human fetal gut (15) (Fig. 1A). Among these, eight regions were marked by only one feature, one region by two and two regions by all three features (Table 1). For *in vitro* functional tests of these elements, we cloned them individually into a pGL4.23 luciferase vector with a minimal TATA-box of the β-globin gene and transfected them into the human neural crest-derived neuroblastoma cell line SK-N-SH. We have previously demonstrated that SK-N-SH expresses *EDNRB* and all other components of the *RET* GRN and is a model system for studies of transcriptional regulation in the ENS (7). For regions with multiple features, we used the overlap between their peaks to define the region of interest (Table 1). As shown in Figure 1B, the genomic elements E1 (3.5-fold; $P = 2 \times 10^{-3}$), E4 (1.8-fold; $P = 1 \times 10^{-3}$), E7 (8.2-fold; $P = 1.9 \times 10^{-11}$), E9 (4.8-fold; $P = 3.1 \times 10^{-8}$) and E10 (3.5-fold; $P = 7.1 \times 10^{-5}$) had significantly higher relative luciferase activity when compared to the basal promoter-only vector and represent five candidate fetal gut *EDNRB* enhancers. Element E10 overlaps the *EDNRB* transcriptional start site and appears to contain the potential promoter. Of these, the strongest enhancer activity was driven by E7, which overlaps a DHS peak and H3K27ac and H3K4me1 epigenetic marks.

TFs regulating EDNRB

The specificity of enhancer function, as measured by its luciferase activity, of each of the 5 putative enhancers required identification of their cognate TFs. We first asked if SOX10, the major *RET* TF (7,16,17) regulates *EDNRB* as well. In the mouse, Sox10 directly regulates *Ednrb* in the developing ENS (18–21) by binding to a 540 bp element upstream of the gene (22, 23). First, we mapped this conserved (>70% base pair similarity between human and mouse) sequence to the human genome and discovered it mapped to E10, the potential *EDNRB* promoter (Fig. 2A). Second, we performed chromatin immunoprecipitation followed by quantitative polymerase chain reaction (ChIP-qPCR) in SK-N-SH for SOX10 to detect strong binding (19-fold enrichment; $P = 6 \times 10^{-3}$) to the SOX10 motif within this conserved sequence. Third, we demonstrated binding specificity by siRNA-mediated *SOX10* knockdown and observing a 3-fold decrease ($P = 2 \times 10^{-3}$) in binding to the same sequence (Fig. 2A).

The common SOX10 regulator of *RET* and *EDNRB* prompted us to search for other shared TFs. We utilized published ChIP-seq data from the ENCODE project (24) to find that element E1 was bound by GATA2, RAD21 and CTCF, E4 by STAT3, E9 by GATA2 and E10 by CTCF and EZH2; we could not identify any known TF binding to element E7 in any of the ENCODE cell lines (24). Of these, GATA2 was of greatest interest because we have previously shown that this TF regulates *RET* and that a variant *RET* enhancer that fails to bind GATA2 is associated with HSCR (7).

For confirmation, we performed ChIP-qPCR for GATA2 in SK-N-SH cells for elements E1 and E9. To test for specificity, we showed that GATA2 strongly binds enhancer E9 with 26-fold enrichment over control IgG ($P = 0.001$) with a 2-fold decrease in binding with *GATA2* knockdown using siRNA ($P = 0.02$) (Fig. 2B). We could not detect any binding of GATA2 at the E1 element as compared to the background in our assays, in contrast to ENCODE data (Fig. 2B). One potential reason for this discrepancy is that the ENCODE ChIP assays in SK-N-SH were performed using a different GATA2 antibody (http://antibodyregistry.org/search.php?q=AB_2616054).

Element E7 had the strongest reporter activity, was marked by all three epigenetic features and yet had no recognizable cognate TF in published data. We searched for binding sites within the E7 sequence using FIMO (25) and 890 validated TF motifs available in public motif databases, specifically the TRANSFAC motif matrix (26–29). We used the setting of "minimize false positives" to detect that only NKX2.5 (TCAAGTG; $P = 1.3 \times 10^{-6}$) and NF-κB (GGAAATTCCC; $P = 0.008$) had a matrix similarity and core similarity score of 1. The matrix similarity is a score that describes the quality of a match between a matrix and an arbitrary part of the input sequence. Analogously, the core similarity denotes the quality of a match between the core sequence of a matrix (i.e. the five most conserved positions within a matrix) and a part of the input sequence. No other TF had a matrix similarity score over 0.5, and the next best score was 0.45 for the TF *AP1* within this sequence.

Of these, NKX2.5 was of primary interest because, although it is primarily a TF controlling early mesoderm differentiation and cardiac tissue morphogenesis in vertebrates, it also has a role in patterning in gut morphogenesis (30,31). In the mouse, *Nkx2.5* along with *Gata3* and *Sox9* are expressed in undifferentiated cells in the pyloric mesenchyme, and loss of *Nkx2.5* or *Gata3*

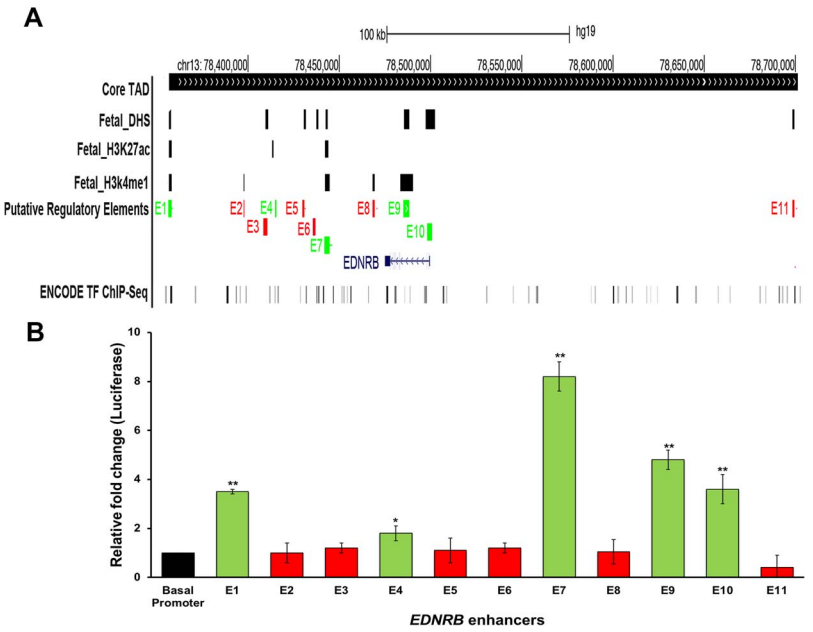

Figure 1. Identifying putative enhancers at the EDNRB locus. (**A**) A 350 kb genomic segment comprising the core TAD in eight human cell lines containing 11 putative CREs defined using ENCODE DHS and H3K4me1 or H3K27ac marks from a 108-day-old human fetal intestine. The locations of all ENCODE TF ChIP-seq sites and the *EDNRB* gene are indicated. (**B**) *In vitro* luciferase assays in SK-N-SH cells show significant enhancer activity in 5 of the 11 putative CREs (marked in green) compared to a promoter-only control. Error bars represent SEs of the mean (*$P < 0.01$, **$P < 0.001$) for three independent biological replicates for each luciferase assay.

Table 1. Eleven potential regulatory elements (hg19 coordinates) within a 341 kb *EDNRB* TAD marked by H3Kme1, H3K27ac and DHS marks in human fetal large intestine

Element (size)	hg19 coordinates	Epigenomic marks
E1 (1587 bp)	chr13: 78353421-78 355 008	DHS, H3K4me1, H3K27ac
E2 (654 bp)	chr13: 78 394 428-78 395 082	H3K4me1
E3 (1853 bp)	chr13: 78 406 337-78 408 190	DHS
E4 (777 bp)	chr13: 78 410 031-78 410 808	H3K27ac
E5 (1217 bp)	chr13: 78 427 391-78 428 608	DHS
E6 (1253 bp)	chr13: 78 434 192-78 435 445	DHS
E7 (1054 bp)	chr13: 78439541-78 440 595	DHS, H3K4me1, H3K27ac
E8 (1111 bp)	chr13: 78 465 330-78 466 441	H3K4me1
E9(1322 bp)	chr13: 78 481 415-78 482 733	DHS, H3K4me1
E10 (1313 bp)	chr13: 78 493 407-78 494 720	DHS
E11 (1125 bp)	chr13: 78 695 152-78 696 277	DHS

These *cis* elements were assayed for enhancer activity in SK-N-SH cells; elements demonstrating significant activity over the basal promoter-only construct are marked in bold.

alters sphincter morphology, resulting in severe hypoplasia of a particular dorsal fascicle of longitudinal smooth muscles in the gut (32). Although NF-κB is also ubiquitously expressed in the developing gut and plays a significant role in the regulation of intestinal epithelial homeostasis and inflammation (33–35), it has no reported role in gut morphogenesis. We performed ChIP-qPCR for both NKX2.5 and NF-κB in SK-N-SH cells, independently, and detected significant binding (12-fold enrichment; $P = 0.001$) for NKX2.5 but no binding of NF-κB to E7 (0.28-fold enrichment; $P = 0.8$) (Fig. 2C). Additionally, we also demonstrated that NKX2.5 binding to E7 was reduced 3.6-fold ($P = 8 \times 10^{-3}$) under siRNA-mediated knockdown of NKX2.5 in SK-N-SH cells (Fig. 2C).

To prove that the identified TFs do indeed control *EDNRB* expression, we performed siRNA-mediated knockdown of each TF in SK-N-SH cells and measured both the TF transcript level and *EDNRB* gene expression, using Taqman-based qPCR assays. These data showed that *EDNRB* expression was indeed reduced by 38% ($P = 4 \times 10^{-4}$), 24% ($P = 2.3 \times 10^{-3}$) and 32% ($P = 3.1 \times 10^{-3}$) consequent to the knockdown of *SOX10*, *GATA2* and *NKX2.5* genes, respectively; as a control, knockdown of *EDNRB* by its specific siRNA reduced its expression 78% ($P = 6.4 \times 10^{-6}$) (Fig. 3A). Thus, each of these TFs control *EDNRB* gene expression (Fig. 3A). In contrast, knockdown of *RARB*, the remaining known *RET* TF (7), had no effect on *EDNRB* expression (Fig. 3A). For completeness, we checked whether *RET* expression was perturbed in *NKX2.5* siRNA treated cells, as compared to control cells, and observed no change in gene expression (Supplementary Fig. 1). Thus NKX2.5 is an independent TF for *EDNRB* unlike SOX10 and GATA2.

We conducted additional tests to demonstrate that loss of each cognate TF leads to loss of enhancer activity. Specifically, we performed luciferase assays in SK-N-SH cells independently transfected with siRNAs against *GATA2*, *SOX10*, *NKX2.5* or a negative control, to assess the activity of each putative enhancer. E1 did not show any loss of activity; E9 showed a 2-fold decrease in

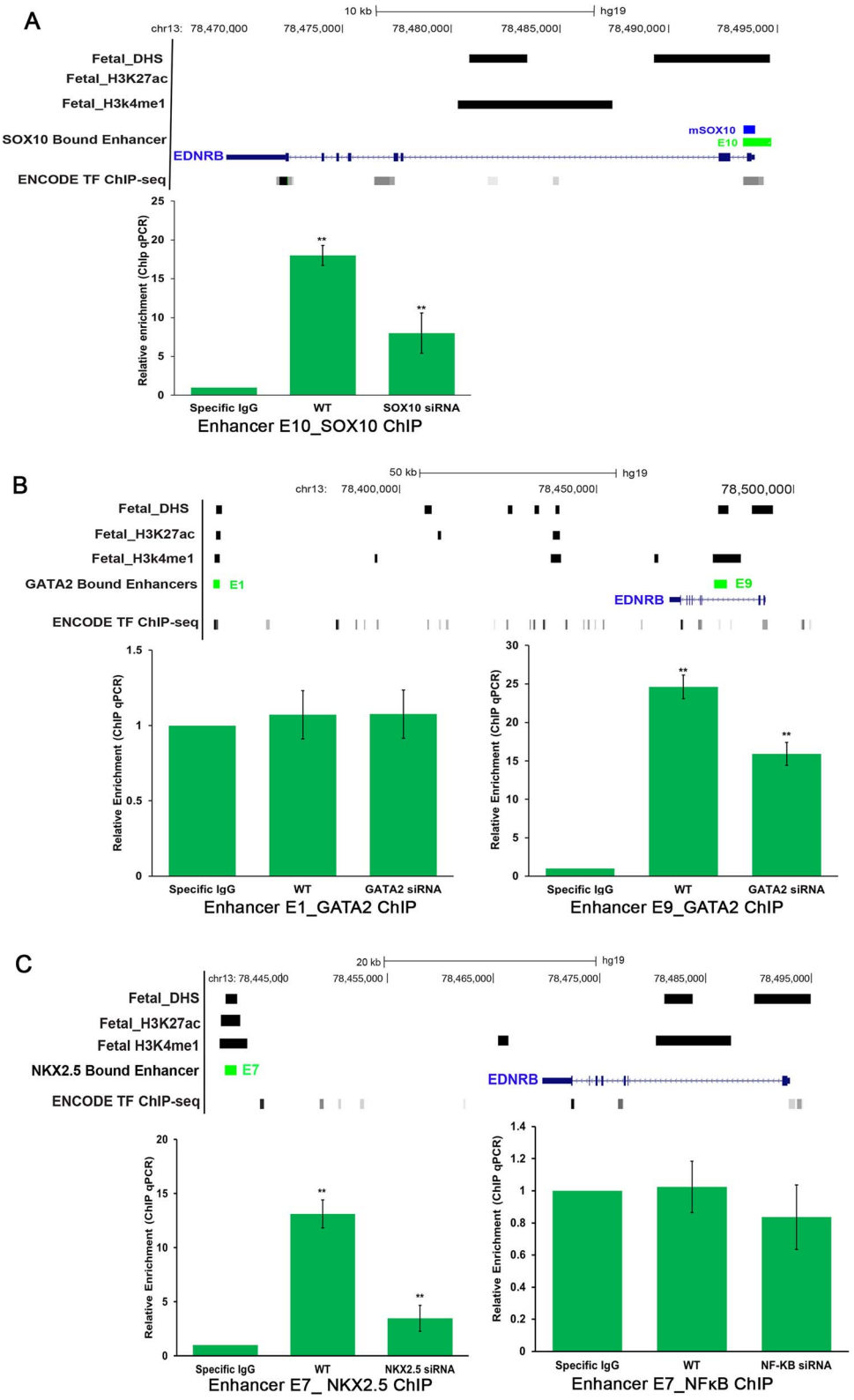

Figure 2. Identification of the cognate TFs bound to EDNRB enhancers. (**A**) Genomic map of the *EDNRB* locus with location for element E10 and ChIP-qPCR assays using a SOX10 antibody show enrichment of binding as compared to the background in SK-N-SH cells. The specificity of this binding is shown by siRNA knockdown of *SOX10* with a concomitant reduction in the ChIP-qPCR signal. (**B**) Analogous assays for two putative GATA2 enhancers (E1 and E9) and ChIP-qPCR assays using a GATA2 antibody show enrichment of binding to E9 but not E1. (**C**) ChIP-qPCR assays on enhancer region E7 demonstrate specific binding of NKX2.5 but not NF-κB. Error bars represent SEs of the mean (*$P < 0.01$, **$P < 0.001$) for three independent biological replicates for each ChIP.

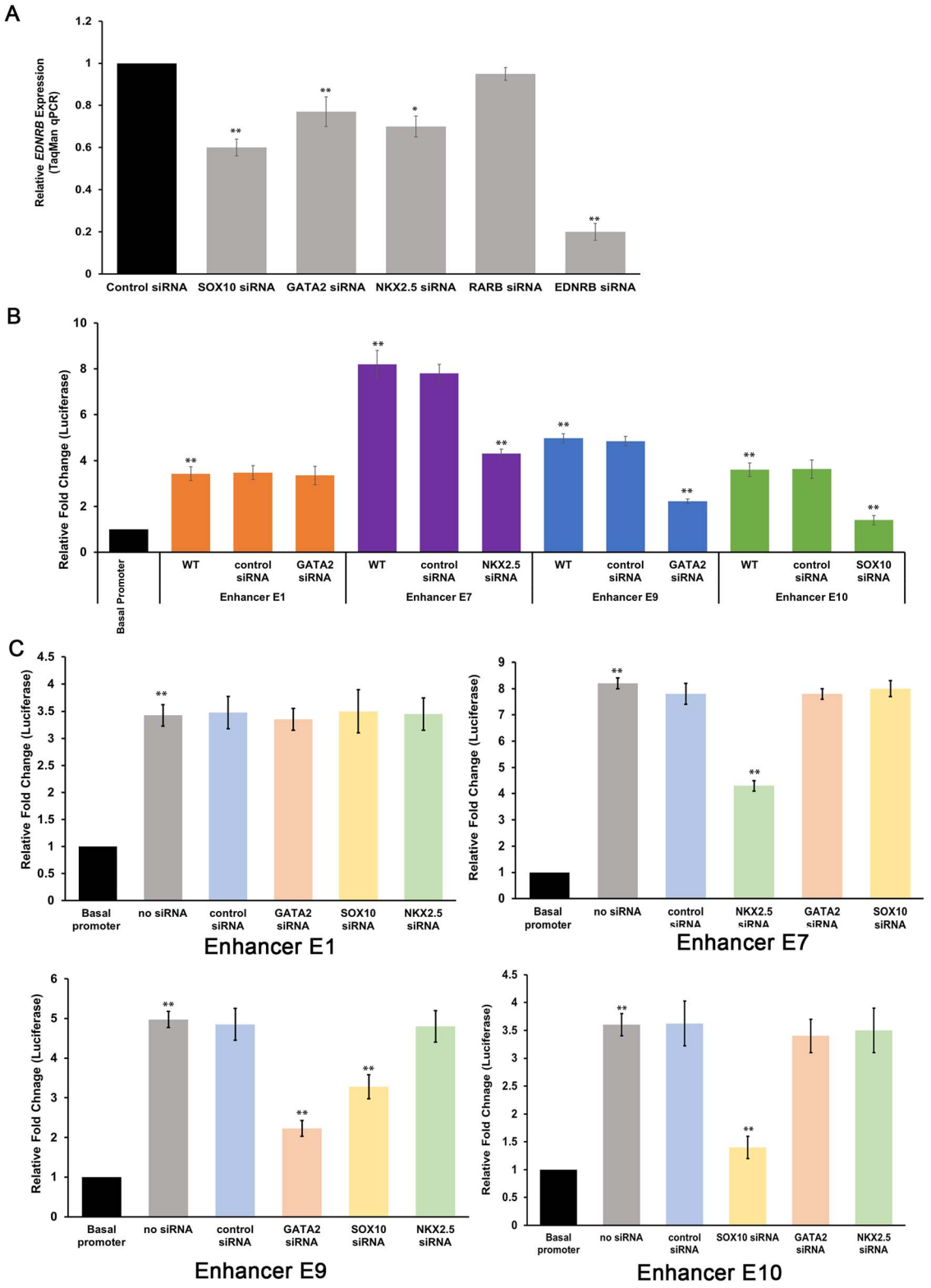

Figure 3. TF-mediated *in vitro* control of gene expression. (**A**) siRNA-mediated knockdown of *SOX10*, *GATA2* and *NKX2.5* but not *RARB* in SK-N-SH cells downregulates *EDNRB* transcription. (**B**) siRNA-mediated knockdown of GATA2 affects activity of enhancer E9 but not E1, further confirming GATA2 binding to E9 only. Similar experiments, including using control siRNAs, show the specificity of binding of NKX2.5 and SOX10 to E7 and E10, respectively. (**C**) siRNA-mediated knockdown of GATA2, SOX10 and NKX2.5 demonstrates that loss of SOX10 also has an effect on activity of GATA2 regulated enhancer E9, highlighting feedback between the two TFs. The other enhancers are only affected by loss of their cognate TF. Pairwise comparisons are against a vector with basal promoter-only (black) for measuring enhancer activity and between untransfected and siRNA transfected cells for measuring TF specificity for both (B) and (C). Error bars represent SEs of the mean (*$P < 0.01$, **$P < 0.001$) for five independent biological replicates in all experiments.

activity ($P = 2.7 \times 10^{-3}$), E7 a 1.9-fold drop in activity ($P = 10^{-4}$) and E10 a 2.5-fold decrease ($P = 3.8 \times 10^{-4}$), when *GATA2*, *NKX2.5* and *SOX10* were knocked down, respectively (Fig. 3B). Thus, except for E1, the E7, E9 and E10 elements are enhancers that bind specific TFs and regulate *EDNRB* gene expression.

To test if there is a combinatorial activity and feedback between enhancers via the TFs, we also quantified the luciferase activity of each enhancer by knocking down all the TFs (*GATA2*, *SOX10* and *NKX2.5*) independently with their cognate siRNAs. While enhancer E1 showed no effect, E7 and E10 had effects only when their cognate TFs, i.e. NKX2.5 and SOX10, respectively, were knocked down but showed no effects when other TFs were attenuated (Fig. 3C). Only GATA2 bound E9 enhancer showed a 1.5-fold decrease ($P = 1.3 \times 10^{-2}$) in activity when *SOX10* was knocked down (Fig. 3C), highlighting a feedback, either direct or indirect between *SOX10* and *GATA2* in SK-N-SH cells.

In vivo effect of Sox10 in the developing mouse gut

Transcriptional studies in *in vitro* cell culture models are limited by the absence of multiple cells and tissue types, which plays a critical role in transcriptional regulation *in vivo*. To examine if our detected effect of *SOX10* on *EDNRB* transcription *in vitro* is recapitulated *in vivo* during ENS development, we used a heterozygous *Sox10* knockout mouse, which also develops aganglionosis (36,37). Multiple studies have previously demonstrated that *Sox10* and *Ednrb* are epistatic in the developing mouse gut most likely through direct control of its transcription during ENCC migration and differentiation (18–22). We assayed for *Ednrb*, *Sox10*, *Gata2*, *Nkx2.5* and *Ret* gene expression using Taqman-based qPCR in the developing mouse gut at E11.5 and E12.5, when the ENCCs cross the cecum and enter the colon. As expected, *Sox10* is expressed at 50% levels, as compared to wild-type embryos at both stages, whereas *Ednrb* expression is also reduced by 30% at E11.5 ($P = 3 \times 10^{-5}$) and by 40% at E12.5 ($P = 2.2 \times 10^{-5}$). Additionally, we also detected 32% ($P = 0.002$) and 60% ($P = 2.4 \times 10^{-5}$) reduction in *Gata2* expression at E11.5 and E12.5, respectively, recapitulating the Sox10-Gata2 feedback we had observed in SK-N-SH cells. There was also a 21% ($P = 0.001$) reduction in *Nkx2.5* expression but only at E12.5. Expectedly, *Ret* gene expression is reduced by 40% at E11.5 ($P = 3.6 \times 10^{-5}$) and 50% ($P = 2.5 \times 10^{-6}$) at E12.5 in the *Sox10* null heterozygote mouse gut, as we demonstrated previously (7) (Fig. 4). These results highlight that *Sox10* not only controls the expression of *Ednrb* and *Ret* but also *Gata2* and *Nkx2.5* in a developmental stage-specific manner. Thus, a common regulatory network involving *Ret* and *Ednrb*, in the developing ENCC during enteric neurogenesis, is driven by *Sox10* and *Gata2* TFs.

Transcriptional feedback in the RET–EDNRB GRN

Every GRN is uniquely defined by the interactions between its constituent genes. Thus, we directly tested for feedback between *EDNRB*, *RET* and their TFs and tested whether this control was *EDNRB* dose-dependent. We varied *EDNRB* expression by varying the concentration of *EDNRB* siRNA and quantified the gene expression of *SOX10*, *GATA2*, *NKX2.5*, *RARB*, *EDNRB* and *RET* in SK-N-SH cells by Taqman qPCR (Fig. 5A). *EDNRB* siRNA concentrations up to 15 μM led to a maximum of 16% ($P = 0.01$) reduction, and concentrations up to 17 μm led to a maximum of 45% ($P = 0.008$) reduction in *EDNRB* expression but with no measurable expression changes in the other genes. However, at a concentration of 25 μM siRNA, *EDNRB* levels were reduced by 88% ($P = 6.5 \times 10^{-7}$), and expression of *RET*, *SOX10* and *GATA2* reduced by 32% ($P = 0.006$), 32% ($P = 0.004$) and 20% ($P = 0.004$), respectively. At 40 μM siRNA, the levels of *EDNRB* were reduced by ∼90% ($P = 2.7 \times 10^{-8}$), while *RET*, *SOX10* and *GATA2* expression were unchanged as compared to the 25 μM siRNA dose; *NKX2.5* and *RARB* levels remain unchanged throughout this concentration range having no effect from loss of *EDNRB* expression. It is interesting to note that, although there is reduced expression of SOX10, due to reduced EDNRB expression, this does not affect the levels of NKX2.5, even though we have observed *Sox10* control of *Nkx2.5* in the mouse gut at E12.5. We believe that there are two likely explanations: (1) there are additional regulatory controls on NKX2.5 in SK-N-SH cells as compared to the gut, and (2) the effect we see in the gut is developmental time-specific, which cannot be modeled in cultured cells. Thus, there is a positive dose-dependent feedback of *EDNRB* on the transcription of two of its TFs and *RET*, highlighting the bidirectionality of transcriptional control which lies at the heart of many regulatory networks.

Since *EDNRB* expression affects *RET* transcript levels as well, we investigated if the converse was true. We varied *RET* gene expression by varying the concentration of *RET* siRNA and quantified gene expression of the same genes as in the above (Fig. 5B). *RET* siRNA concentrations up to 15 μM led up to 50% reduction in *RET* gene expression ($P = 2.35 \times 10^{-5}$) with no significant loss of *EDNRB* expression. However, when *RET* siRNA concentration increased to 17 μM and 25 μM, *RET* expression further decreased to 25% ($P = 4.1 \times 10^{-8}$) and ∼0% ($P = 7.2 \times 10^{-9}$), respectively, while *EDNRB* gene expression decreased to 80% at both levels ($P = 0.003$ at 17 μM and $P = 0.0023$ at 25 μM). Similarly, there was no change in *SOX10* and *GATA2* up to 15 μM of *RET* siRNA. *SOX10* expression levels decreased more slowly to 80% ($P = 0.05$) and 20% ($P = 2.0 \times 10^{-9}$), respectively, while *GATA2* decreased to 70% at 17 μM ($P = 8 \times 10^{-3}$) and 50% at 25 μM ($P = 5.3 \times 10^{-3}$). *RARB* and *NKX2.5* levels were unchanged due to loss of *RET* expression.

Discussion

This study demonstrates that the two major genes controlling early ENS development and whose functional loss is associated with HSCR, *RET* and *EDNRB* are coregulated within one GRN. Specifically, although multiple enhancers regulate each gene (*RET*: 10 known, (7); *EDNRB*: 5 known, this study), the TFs GATA2 and SOX10 regulate both of them while *RET* and *EDNRB* demonstrate dose-dependent feedback on these same TFs, as well as on other genes within the GRN, at least in SK-N-SH cells. This bidirectional regulatory control common to both genes is the most parsimonious explanation for the strong epistasis between *RET* and *EDNRB* mutations observed in human and mouse aganglionosis (11,12) (Fig. 6).

Our study demonstrates that transcriptional feedback between *EDNRB* and its TFs is evident only when *EDNRB* gene expression levels fall below 50% (i.e. heterozygote levels). These results can therefore explain why, in the mouse, *Ednrb* hypomorphic and null mutations show aganglionosis penetrance only when its relative expression is <50% (38,39). Further, because *Ednrb* hypomorphic and null mutations show pigmentary anomalies arising from melanocytes but not aganglionosis in heterozygotes, the *Ednrb* gene dosage effect is probably absent in melanocytes. In other words, the effect of *Ednrb* loss of function mutations and its effect on the *Ret–Ednrb* GRN are cell-type specific in the mouse; hence, the same mutation will have different consequences in different cells. Our previous study of a *EDNRB* W276C hypomorphic mutation in HSCR in an Old

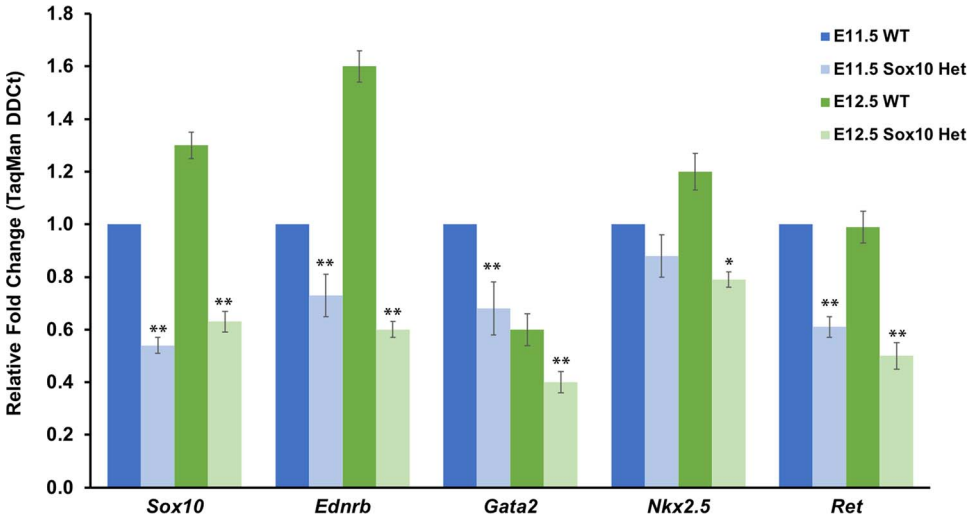

Figure 4. RET–EDNRB GRN in the developing mouse ENS. Gene expression of *Ednrb*, *Gata2*, *Nkx2.5* and *Ret* in the developing mouse gut at embryonic stage E11.5 and E12.5 in wild-type and *Sox10* heterozygote embryos shows that *Ednrb*, *Gata2* and *Ret* are transcriptionally affected at both developmental stages by loss of *Sox10* expression. The effect on *Nkx2.5* is only observed at E12.5. All pairwise comparisons are between wild-type and heterozygous embryonic guts within each developmental stage. Error bars represent SEs of the mean (*$P < 0.01$, **$P < 0.001$) for three independent embryos for each developmental stage and genotype.

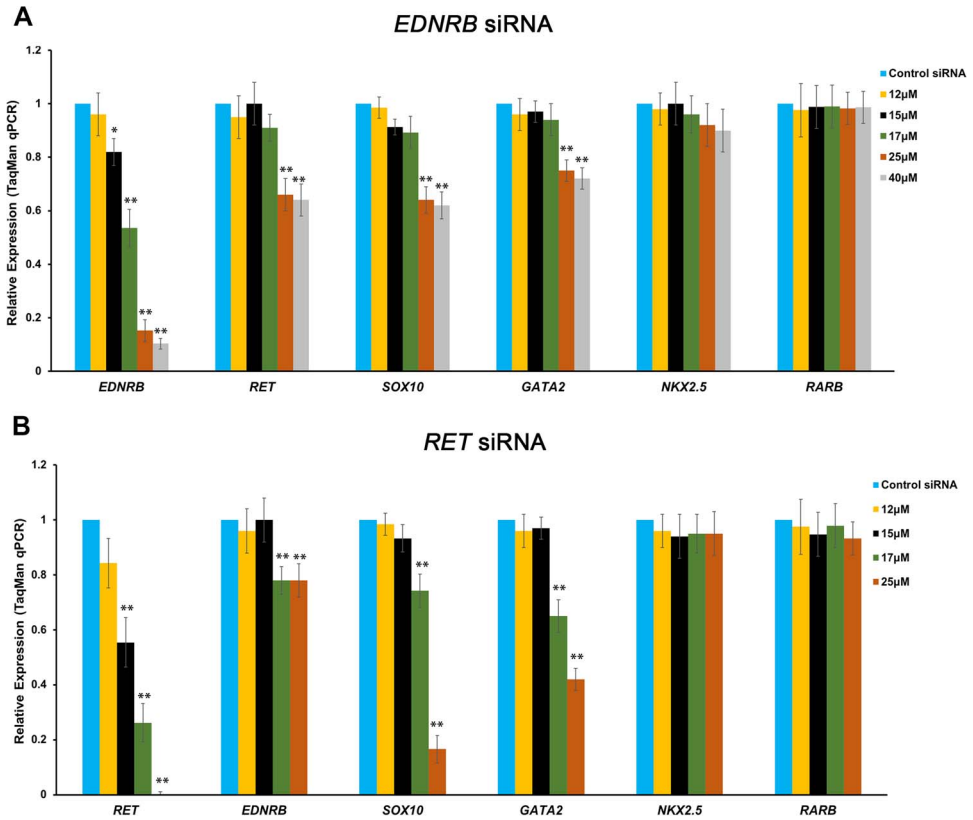

Figure 5. Transcriptional feedback between RET, EDNRB and their TFs. (**A**) *EDNRB* gene expression in human SK-N-SH cells with increasing doses of *EDNRB* siRNA (12–40 μM). The transcriptional effect is seen in *RET*, *SOX10* and *GATA2* when *EDNRB* levels are significantly reduced to below 50% of wild-type levels. (**B**) Experiments as in (A) for *RET* loss of expression (12–25 μM) in SK-N-SH cells show a transcriptional feedback on *EDNRB*, *SOX10* and *GATA2* but only when *RET* expression falls below 50% of wild-type levels. *NKX2.5* and *RARB* levels remain unchanged in both experiments. All pairwise comparisons are with transfections using control siRNAs. Error bars represent SEs of the mean (*$P < 0.01$, **$P < 0.001$) for five independent biological replicates.

Order Mennonite population, where its high frequency leads to both mutant heterozygotes and homozygotes, demonstrates dosage-dependent phenotypic defects analogous to the mouse (40). However, human *EDNRB* W276C heterozygotes, unlike the mouse, can also display aganglionosis, which likely results from a common SOX10-binding enhancer allele regulating both *RET* and *EDNRB* that segregates in the Old Order Mennonite population and predisposes to HSCR (40). Thus, parsimony

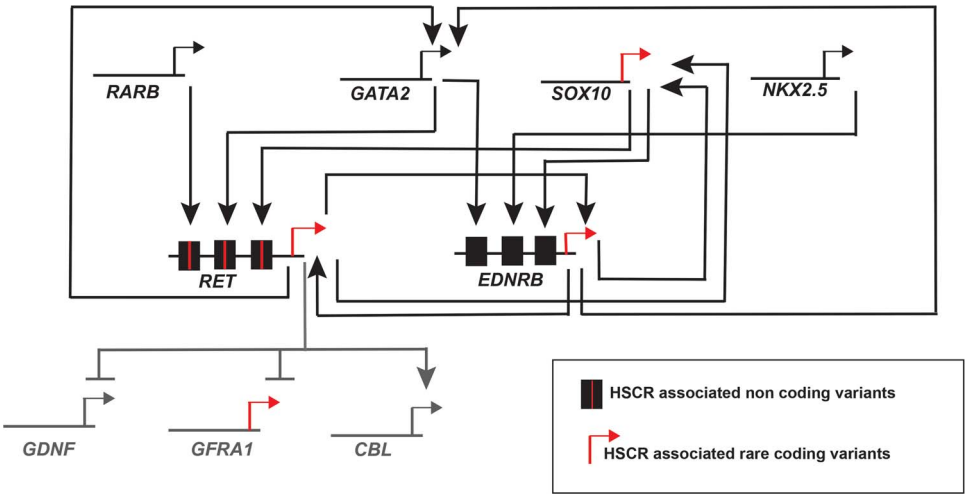

Figure 6. The RET–EDNRB GRN. RET and *EDNRB* are the two major genes for ENS development and harbor multiple mutations leading to HSCR. These genes are coregulated within a larger GRN controlled by at least two common TFs with feedback and feed forward loops as significant features. The grey colored components of the GRN (*GDNF*, *GFRA1* and *CBL*) were deciphered in our previous study (7).

dictates that the *RET–EDNRB* GRN is also cell-type specific in the human.

The effect of GATA2 and SOX10 on *RET* and *EDNRB* is minimally through the enhancers we have experimentally defined in SK-N-SH cells. However, the mechanism by which RET and EDNRB interact with GATA2 and SOX10 is unknown. This is unlikely to be through the canonical tyrosine kinase or G-protein coupled receptor signaling pathways since the genes in the *RET* signaling cascade are unaffected by siRNA knockdown in SK-N-SH cells or in the *Ret* null mutant homozygote mouse (7). We suspect that this is owing to specific posttranslational modifications of SOX10 and GATA2, in response to their lower expression, inhibiting their nuclear entry or making it inefficient. SOX10 is a nucleo-cytoplasmic shuttle protein and so provides some credence to this hypothesis (41).

We also hypothesize that sequence variants in at least the GATA2 and SOX10 binding enhancers, E9 and E10, would be HSCR-associated, but no such variants have been identified to date. Note that in the European ancestry population (42) a minimum of 146 polymorphisms (minor allele frequency [MAF], ≥1%) exist in the 11 putative enhancers reported here, 37 of which are in the 5 experimentally proven elements. The absence of associations refers to common (MAF, ≥10%) variants that have been tested (43,44). Rare variants could still be HSCR-associated, but identifying these will require more comprehensive studies.

Finally, for HSCR and gut development, gene expression of *RET* and *EDNRB* requires the activity of other TFs and enhancers involved, such as RARB and NKX2.5, and others yet to be identified. Thus, the *RET–EDNRB* GRN controlling ENS migration and differentiation, which currently comprises nine genes is undoubtedly much bigger. Note that *EDNRB*, *GATA2* and *SOX10* are expressed very early during neural crest cell specification and migration (45) and, subsequently, all the way through ENS development. Therefore, it is likely there would be both cell-type specific and cell-type invariant GRNs centered on these genes, as have been reported in melanocytes, migrating neural crest cells and HeLa cells (23). At the same time, loss of *Ret* expression in the developing ENS leads to hundreds of genes being affected (7). It is, therefore, not inconceivable that many genes jointly regulate *RET* and *EDNRB* and are commonly affected by their loss of function, and indeed, some of the observed effect on transcription could be mediated indirectly through other genes we have not uncovered yet. Thus, the GRN we have discovered is only the core of the network which involves multiple genes mutated in HSCR (Fig. 6) but is incomplete and clearly much bigger than what we have deciphered. Expanding the GRN would also shed light on other genes affected by and controlled by the specific TFs we have uncovered here and lead to a better understanding of how these interactions are wired. In other words, understanding the effect of sequence variation in ENS genes involved in HSCR and other neurocristopathies will require elucidating and understanding this dynamic GRN.

Materials and Methods

TAD definition and ChIP-seq peak calling

We utilized published HiC data (14) at the *EDNRB* locus from eight human cell lines and used Juicebox (46) to construct TADs by mapping the normalized data for each cell type at 5 kb resolution. The genomic coordinates (hg19) for TADs around *EDNRB* in each cell type are as follows: GM12878 (Chr13:78360000-78 700 000), HMEC (Chr13:78325000-79 865 000), HUVEC (chr13:78355000-78 700 000), IMR90 (chr13:78345000-78 700 000), K562 (Chr13:78705000-79 605 000), KBM7 (Chr13:78345000-78 705 000) and NHEK (Chr13:78350000-78 695 000). The common core TAD between these cells lines is a 341 kb region (Chr13:78359528-78 701 413).

Three epigenomic data sets from a 108-day-old human fetal large intestine, histone H3K27ac ChIP-seq (GSM1058765), histone H3K4me1 ChIP-seq (GSM1058775), and DNaseI-seq (GSM817188) were downloaded from the NIH Roadmap Epigenomics Project (http://www.roadmapepigenomics.org/data/tables/fetal). For each data set, MACS software v1.4 (47) with default settings was used to call "peaks" where sequence reads were significantly enriched. With the default peak-calling threshold ($P < 10^{-5}$), 51 771, 61 689 and 66 930 genomic regions were identified in GSM1058765, GSM1058775, and GSM817188 respectively.

Regulatory element selection

Within the core TAD, we defined potential regulatory elements as segments overlapping peaks for any of the two histone marks or DHS; with multiple peaks, we used the overlap region. For region E9, which had a 3.9 kb overlap, we used the 1.3 kb region centered on the peak to keep all tested fragment sizes similar. For region E10, which overlapped a 5.7 kb DHS peak, we used the 1.3 kb fragment centered on the peak and overlapping the transcription start site of *EDNRB*.

Cell lines

The human neuroblastoma cell SK-N-SH, purchased from ATCC (no. HTB-11), was grown under standard conditions (DMEM +10% FBS and 1% penicillin streptomycin).

Reporter assays

Four hundred nanograms of firefly luciferase vector (pGL4.23, Promega Corporation) containing the DNA sequence of interest and 2 ng of Renilla luciferase vector (transfection control) were transiently transfected into cell line SK-N-SH ($5–6 \times 10^4$ cells/well), using 6 ml of FuGENE HD transfection reagent (Roche Diagnostic, USA) in 100 ml of OPTIMEM medium (Invitrogen, USA). The cells were grown for 48 h, and luminescence was measured using a Dual Luciferase Reporter Assay System on a Tecan multidetection system luminometer, per the manufacturer's instructions. To check for the effect of loss of specific TFs on the reporter assay, we transfected cells with *SOX10* siRNA (L-017192-00), *GATA2* siRNA (L-009024-02), *NKX2.5* siRNA (L-019795-00-0005) or a negative control non-targeting siRNA (D-001810-10) (Dharmacon) at a concentration of 25 μM for 24 h prior to transfecting the corresponding enhancer construct. All assays were performed in triplicate with independent readings (n = 9): the data presented are the means with their standard errors (SEs).

ChIP-qPCR assays

ChIP was performed thrice independently for each antibody using 1×10^6 SK-N-SH cells for each TF using the EZ-Magna ChIP kit (Millipore), as per the manufacturer's instruction, with the following modifications: the chromatin was sonicated for 30 s on and 30 s off for 10 cycles; sheared chromatin was preblocked with unconjugated beads for 4 h; and specific antibodies were separately conjugated to the beads for 4 h before immunoprecipitation was performed with the preblocked chromatin. The following antibodies were used: SOX10 (sc-17 342X, Santa Cruz), 10 mg; GATA2 (ab22849, Abcam), 8 mg; NKX2.5 (ab106923, Abcam), 5 mg; and NF-κB (17–10 060, Millipore Sigma), 5 mg. ChIP assays were also performed on cells 48 h after transfection with the following siRNAs at 25 μM to assess the specificity of TF binding: SOX10 (L-017192-00), GATA2 (L-009024-02) and NKX2.5 (L-019795-00-0005) (Dharmacon). qPCR assays were performed using SYBR green (Life Technologies) and specific primers against the E1 (E1_Fwd 5' CAAGAGGAAGTGCTGCCCTG 3'; E1_Rev 5' GCCTCTCTCAAGCACCTGAG 3'), E7 (*E7_Fwd 5' CCCCAAGTATCAAGTGTAGCAGT 3'; E7_Rev 5' GATACATGATGTGTGCCCGA 3'*), E9 (*E9_Fwd 5' AGCTCTGCACTGAATCCAGG 3'; E9_Rev 5' CAGGCCTCCAGTGGTATGAA 3'*) and E10 (*E10_Fwd 5' TCCCTTCCCATCAATCACCG 3'; E10_Rev 5' ACTGATGCTGTCCAGGCATC 3'*) regions. The data were normalized to input DNA, and enrichment was calculated by fold excess over ChIP performed with specific IgG as background signal. All assays were done in triplicate for each independent ChIP assay (n = 9).

Sox10 mouse

The generation of *Sox10^{lacZ}* mice has been described previously (36). Heterozygous mice were intercrossed to generate all possible genotypes, and embryonic guts at E11.5 and E12.5 were dissected and genotyped; male embryonic guts were selected for further analysis. The tissues were washed in ice-cold phosphate buffered saline and snap frozen in liquid nitrogen for RNA extraction. Genotyping was performed on yolk sac DNA using primers specific to the *Sox10* locus (Sox10Fwd: 5'-*CAGGTGGGCGTTGGGCTCTT-3'* and Sox10Rev: 5'-*CAGAGCTTGCCTAGTGTCTT-3'*; 506 bp amplicon) for wild-type embryos and the lacZ transgene (LacZFwd: 5'-*CTGGCAGGCGTTTCGTCAGTATCC-3'* and 5'-*AGCGACATCCAGAGGC ACTTCACCC-3'*; 364 bp amplicon) for mutants. Genotyping for sex used primers mapping to the *Kdm5c/d* genes (Kdm5Fwd: 5'-*CTGAAGCTTTTGGCTTTGAG-3'* and Kdm5Rev: 5'-*CCGCTGCCAAAT TCTTTGG-3'*) resulting in two 331 bp bands specific for the X chromosome and an additional 301 bp Y chromosome band (48). All animal studies were reviewed and approved by the Institutional Animal Care and Use Committee of Johns Hopkins University (Protocol MO12M374) where these experiments were performed.

siRNA assays

EDNRB (L-003657-00-0005), *RET* (L-003170-00-0005), *SOX10* (L-017192-00), *GATA2* (L-009024-02), *NKX2.5* (L-019795-00-0005) and *RARB* (L-003438-02) SMARTpool siRNAs (a combination of four individual siRNAs targeting each gene) along with ON-TARGET plus non-targeting siRNAs (D-001810-10, negative control) (Dharmacon, USA) were transfected at concentration ranges of 12 to 40 μM in SK-N-SH cells at a density of 10^4–10^5 cells using FuGene HD Transfection reagent (Promega Corporation, USA) per the manufacturer's instructions. Negative control siRNAs were always transfected at 25 μM concentration. To measure the efficacy of each gene specific siRNAs, we did a titration of each siRNA and measured gene expression by Taqman qPCR for its cognate gene. For *SOX10*, adding 15 μM, 17 μM and 25 μM siRNA led to transcript reduction by 28% ($P = 3.2 \times 10^{-3}$), 57% ($P = 1.8 \times 10^{-5}$) and 77% ($P = 2.4 \times 10^{-6}$), respectively. Corresponding assays for *GATA2* led to reduction by 12% ($P = 0.008$), 49% ($P = 2.2 \times 10^{-4}$) and 79% ($P = 1.4 \times 10^{-6}$) and for *NKX2.5*, to reduction by 16% ($P = 0.008$), 40% ($P = 1.2 \times 10^{-4}$) and 72% ($P = 1.3 \times 10^{-5}$), respectively (Supplementary Fig. 2). For ChIP and luciferase assays in which the specific TF was knocked down, we used 25 μM of siRNA. The corresponding titration values for *RET* and *EDNRB* are detailed under results.

Total RNA was extracted from cells 48 h posttransfection and Taqman gene-specific assays conducted as described. Five independent transfections were used for each siRNA, and each Taqman assay was performed in triplicate (n = 15); *P*-values were calculated from pairwise two-tailed *t* tests, and the data were presented as means with their SEs.

Gene expression Taqman assays

Total RNA was extracted from SK-N-SH cells and individual mouse embryonic guts using TRIzol (Life Technologies, USA) and

cleaned on RNeasy columns (QIAGEN, USA). Five hundred micrograms of total RNA was converted to cDNA using SuperScriptIII reverse transcriptase (Life Technologies, USA) using Oligo-dT primers. The diluted (1/5) total cDNA was subjected to Taqman gene expression (ThermoFisher Scientific) using transcript-specific probes and primers (Table S1). Human or mouse β-actin was used as an internal loading control, as appropriate, for normalization. Five independent biological samples for mouse fetal gut at each stage or five independent wells for SK-N-SH cells were used for RNA extraction and each assay performed in triplicate (n = 15). Relative fold change was calculated based on the 2DDCt (threshold cycle) method. For siRNA experiments, 2DDCt for negative control non-targeting control siRNA was set to unity; for measuring gene expression in mice guts, the 2DDCt value for E11.5 wild-type animals was set to unity. *P*-values were calculated from pairwise two-tailed *t* tests, and the data were presented as means with their SEs. Subsequently, *P*-values were calculated from pairwise two-tailed *t* tests, and the data were presented as the mean fold change with its SE.

Supplementary Material

Supplementary Material is available at *HMG* online.

Acknowledgements

The authors gratefully acknowledge the assistance of Dr. William J. Pavan (NHGRI, NIH) and Dr. Michael Wegner (Institut für Biochemie, Friedrich-Alexander-Universitat) for providing *Sox10* mutant mice.

Conflict of Interest statement. None declared.

Funding

This work was supported by a National Institute of Health MERIT award [HD28088 to A.C.].

References

1. Visscher, P.M., Wray, N.R., Zhang, Q., Sklar, P., McCarthy, M.I., Brown, M.A. and Yang, J. (2017) 10 years of GWAS discovery: biology, function, and translation. *Am. J. Hum. Genet.*, **101**, 5–22.
2. Chakravarti, A. and Turner, T.N. (2016) Revealing rate-limiting steps in complex disease biology: the crucial importance of studying rare, extreme-phenotype families. *Bioessays*, **38**, 578–586.
3. Wood, A.R., Esko, T., Yang, J., Vedantam, S., Pers, T.H., Gustafsson, S., Chu, A.Y., Estrada, K., Luan, J., Kutalik, Z. *et al.* (2014) Defining the role of common variation in the genomic and biological architecture of adult human height. *Nat. Genet.*, **46**, 1173–1186.
4. Boyle, E.A., Li, Y.I. and Pritchard, J.K. (2017) An expanded view of complex traits: from polygenic to omnigenic. *Cell*, **169**, 1177–1186.
5. Davidson, E.H. (2006) *The regulatory genome: gene regulatory networks in development and evolution*. Academic Press, Cambridge, MA, USA.
6. Davidson, E.H. (2010) Emerging properties of animal gene regulatory networks. *Nature*, **468**, 911–920.
7. Chatterjee, S., Kapoor, A., Akiyama, J.A., Auer, D.R., Lee, D., Gabriel, S., Berrios, C., Pennacchio, L.A. and Chakravarti, A. (2016) Enhancer variants synergistically drive dysfunction of a gene regulatory network in Hirschsprung disease. *Cell*, **167**, 355–368.e310.
8. Tilghman, J.M., Ling, A.Y., Turner, T.N., Sosa, M.X., Krumm, N., Chatterjee, S., Kapoor, A., Coe, B.P., Nguyen, K.H., Gupta, N. *et al.* (2019) Molecular genetic anatomy and risk profile of Hirschsprung's disease. *N. Engl. J. Med.*, **380**, 1421–1432.
9. Heanue, T.A. and Pachnis, V. (2007) Enteric nervous system development and Hirschsprung's disease: advances in genetic and stem cell studies. *Nat. Rev. Neurosci.*, **8**, 466–479.
10. Barlow, A., de Graaff, E. and Pachnis, V. (2003) Enteric nervous system progenitors are coordinately controlled by the G protein-coupled receptor EDNRB and the receptor tyrosine kinase RET. *Neuron*, **40**, 905–916.
11. Carrasquillo, M.M., McCallion, A.S., Puffenberger, E.G., Kashuk, C.S., Nouri, N. and Chakravarti, A. (2002) Genome-wide association study and mouse model identify interaction between RET and EDNRB pathways in Hirschsprung disease. *Nat. Genet.*, **32**, 237–244.
12. McCallion, A.S., Stames, E., Conlon, R.A. and Chakravarti, A. (2003) Phenotype variation in two-locus mouse models of Hirschsprung disease: tissue-specific interaction between ret and Ednrb. *Proc. Natl. Acad. Sci. U. S. A.*, **100**, 1826–1831.
13. Dixon, J.R., Selvaraj, S., Yue, F., Kim, A., Li, Y., Shen, Y., Hu, M., Liu, J.S. and Ren, B. (2012) Topological domains in mammalian genomes identified by analysis of chromatin interactions. *Nature*, **485**, 376–380.
14. Rao, S.S., Huntley, M.H., Durand, N.C., Stamenova, E.K., Bochkov, I.D., Robinson, J.T., Sanborn, A.L., Machol, I., Omer, A.D., Lander, E.S. *et al.* (2014) A 3D map of the human genome at kilobase resolution reveals principles of chromatin looping. *Cell*, **159**, 1665–1680.
15. Bernstein, B.E., Stamatoyannopoulos, J.A., Costello, J.F., Ren, B., Milosavljevic, A., Meissner, A., Kellis, M., Marra, M.A., Beaudet, A.L., Ecker, J.R. *et al.* (2010) The NIH roadmap epigenomics mapping consortium. *Nat. Biotechnol.*, **28**, 1045–1048.
16. Emison, E.S., McCallion, A.S., Kashuk, C.S., Bush, R.T., Grice, E., Lin, S., Portnoy, M.E., Cutler, D.J., Green, E.D. and Chakravarti, A. (2005) A common sex-dependent mutation in a RET enhancer underlies Hirschsprung disease risk. *Nature*, **434**, 857–863.
17. Emison, E.S., Garcia-Barcelo, M., Grice, E.A., Lantieri, F., Amiel, J., Burzynski, G., Fernandez, R.M., Hao, L., Kashuk, C., West, K. *et al.* (2010) Differential contributions of rare and common, coding and noncoding ret mutations to multifactorial Hirschsprung disease liability. *Am. J. Hum. Genet.*, **87**, 60–74.
18. Bondurand, N., Natarajan, D., Barlow, A., Thapar, N. and Pachnis, V. (2006) Maintenance of mammalian enteric nervous system progenitors by SOX10 and endothelin 3 signalling. *Development*, **133**, 2075–2086.
19. Southard-Smith, E.M., Kos, L. and Pavan, W.J. (1998) Sox10 mutation disrupts neural crest development in Dom Hirschsprung mouse model. *Nat. Genet.*, **18**, 60–64.
20. Stanchina, L., Baral, V., Robert, F., Pingault, V., Lemort, N., Pachnis, V., Goossens, M. and Bondurand, N. (2006) Interactions between Sox10, Edn3 and Ednrb during enteric nervous system and melanocyte development. *Dev. Biol.*, **295**, 232–249.
21. Cantrell, V.A., Owens, S.E., Chandler, R.L., Airey, D.C., Bradley, K.M., Smith, J.R. and Southard-Smith, E.M. (2004) Interactions between Sox10 and EdnrB modulate penetrance and severity of aganglionosis in the Sox10Dom mouse model of Hirschsprung disease. *Hum. Mol. Genet.*, **13**, 2289–2301.
22. Zhu, L., Lee, H.O., Jordan, C.S., Cantrell, V.A., Southard-Smith, E.M. and Shin, M.K. (2004) Spatiotemporal regulation

of endothelin receptor-B by SOX10 in neural crest-derived enteric neuron precursors. *Nat. Genet.*, **36**, 732–737.
23. Watanabe, Y., Stanchina, L., Lecerf, L., Gacem, N., Conidi, A., Baral, V., Pingault, V., Huylebroeck, D. and Bondurand, N. (2017) Differentiation of mouse enteric nervous system progenitor cells is controlled by endothelin 3 and requires regulation of Ednrb by SOX10 and ZEB2. *Gastroenterology*, **152**, 1139, e1134–e1150.
24. Consortium, E.P. (2012) An integrated encyclopedia of DNA elements in the human genome. *Nature*, **489**, 57–74.
25. Grant, C.E., Bailey, T.L. and Noble, W.S. (2011) FIMO: scanning for occurrences of a given motif. *Bioinformatics*, **27**, 1017–1018.
26. Bailey, T.L., Boden, M., Buske, F.A., Frith, M., Grant, C.E., Clementi, L., Ren, J., Li, W.W. and Noble, W.S. (2009) MEME SUITE: tools for motif discovery and searching. *Nucleic Acids Res.*, **37**, W202–W208.
27. Bryne, J.C., Valen, E., Tang, M.H., Marstrand, T., Winther, O., da Piedade, I., Krogh, A., Lenhard, B. and Sandelin, A. (2008) JASPAR, the open access database of transcription factor-binding profiles: new content and tools in the 2008 update. *Nucleic Acids Res.*, **36**, D102–D106.
28. Newburger, D.E. and Bulyk, M.L. (2009) UniPROBE: an online database of protein binding microarray data on protein-DNA interactions. *Nucleic Acids Res.*, **37**, D77–D82.
29. Wingender, E., Dietze, P., Karas, H. and Knuppel, R. (1996) TRANSFAC: a database on transcription factors and their DNA binding sites. *Nucleic Acids Res.*, **24**, 238–241.
30. Lien, C.L., Wu, C., Mercer, B., Webb, R., Richardson, J.A. and Olson, E.N. (1999) Control of early cardiac-specific transcription of Nkx2-5 by a GATA-dependent enhancer. *Development*, **126**, 75–84.
31. Kim, T.H. and Shivdasani, R.A. (2016) Stomach development, stem cells and disease. *Development*, **143**, 554–565.
32. Udager, A.M., Prakash, A., Saenz, D.A., Schinke, M., Moriguchi, T., Jay, P.Y., Lim, K.C., Engel, J.D. and Gumucio, D.L. (2014) Proper development of the outer longitudinal smooth muscle of the mouse pylorus requires Nkx2-5 and Gata3. *Gastroenterology*, **146**, 157–165.e10.
33. Schreiber, S., Nikolaus, S. and Hampe, J. (1998) Activation of nuclear factor kappa B inflammatory bowel disease. *Gut*, **42**, 477–484.
34. Kanther, M., Sun, X., Muhlbauer, M., Mackey, L.C., Flynn, E.J., 3rd, Bagnat, M., Jobin, C. and Rawls, J.F. (2011) Microbial colonization induces dynamic temporal and spatial patterns of NF-kappaB activation in the zebrafish digestive tract. *Gastroenterology*, **141**, 197–207.
35. Wullaert, A., Bonnet, M.C. and Pasparakis, M. (2011) NF-kappaB in the regulation of epithelial homeostasis and inflammation. *Cell Res.*, **21**, 146–158.
36. Britsch, S., Goerich, D.E., Riethmacher, D., Peirano, R.I., Rossner, M., Nave, K.A., Birchmeier, C. and Wegner, M. (2001) The transcription factor Sox10 is a key regulator of peripheral glial development. *Genes Dev.*, **15**, 66–78.
37. Paratore, C., Eichenberger, C., Suter, U. and Sommer, L. (2002) Sox10 haploinsufficiency affects maintenance of progenitor cells in a mouse model of Hirschsprung disease. *Hum. Mol. Genet.*, **11**, 3075–3085.
38. Baynash, A.G., Hosoda, K., Giaid, A., Richardson, J.A., Emoto, N., Hammer, R.E. and Yanagisawa, M. (1994) Interaction of endothelin-3 with endothelin-B receptor is essential for development of epidermal melanocytes and enteric neurons. *Cell*, **79**, 1277–1285.
39. Hosoda, K., Hammer, R.E., Richardson, J.A., Baynash, A.G., Cheung, J.C., Giaid, A. and Yanagisawa, M. (1994) Targeted and natural (piebald-lethal) mutations of endothelin-B receptor gene produce megacolon associated with spotted coat color in mice. *Cell*, **79**, 1267–1276.
40. Puffenberger, E.G., Hosoda, K., Washington, S.S., Nakao, K., deWit, D., Yanagisawa, M. and Chakravart, A. (1994) A missense mutation of the endothelin-B receptor gene in multigenic Hirschsprung's disease. *Cell*, **79**, 1257–1266.
41. Rehberg, S., Lischka, P., Glaser, G., Stamminger, T., Wegner, M. and Rosorius, O. (2002) Sox10 is an active nucleocytoplasmic shuttle protein, and shuttling is crucial for Sox10-mediated transactivation. *Mol. Cell. Biol.*, **22**, 5826–5834.
42. Genomes Project, C., Auton, A., Brooks, L.D., Durbin, R.M., Garrison, E.P., Kang, H.M., Korbel, J.O., Marchini, J.L., McCarthy, S., McVean, G.A. *et al.* (2015) A global reference for human genetic variation. *Nature*, **526**, 68–74.
43. Jiang, Q., Arnold, S., Heanue, T., Kilambi, K.P., Doan, B., Kapoor, A., Ling, A.Y., Sosa, M.X., Guy, M., Jiang, Q. *et al.* (2015) Functional loss of semaphorin 3C and/or semaphorin 3D and their epistatic interaction with ret are critical to Hirschsprung disease liability. *Am. J. Hum. Genet.*, **96**, 581–596.
44. Tang, C.S., Gui, H., Kapoor, A., Kim, J.H., Luzon-Toro, B., Pelet, A., Burzynski, G., Lantieri, F., So, M.T., Berrios, C. *et al.* (2016) Trans-ethnic meta-analysis of genome-wide association studies for Hirschsprung disease. *Hum. Mol. Genet.*, **25**, 5265–5275.
45. Simoes-Costa, M. and Bronner, M.E. (2015) Establishing neural crest identity: a gene regulatory recipe. *Development*, **142**, 242–257.
46. Durand, N.C., Robinson, J.T., Shamim, M.S., Machol, I., Mesirov, J.P., Lander, E.S. and Aiden, E.L. (2016) Juicebox provides a visualization system for hi-C contact maps with unlimited zoom. *Cell Syst.*, **3**, 99–101.
47. Zhang, Y., Liu, T., Meyer, C.A., Eeckhoute, J., Johnson, D.S., Bernstein, B.E., Nusbaum, C., Myers, R.M., Brown, M., Li, W. *et al.* (2008) Model-based analysis of ChIP-Seq (MACS). *Genome Biol.*, **9**, R137.
48. Clapcote, S.J. and Roder, J.C. (2005) Simplex PCR assay for sex determination in mice. *Biotechniques*, **38**, 702, 704, 706.